# Supporting information

## High specific capacitance of a 3D-metal–organic framework confined growth in $CoMn_2O_4$ nanostars as advanced supercapacitor electrode materials

Reza Abazari,[a] Soheila Sanati,[a] Ali Morsali,*[,a] and Deepak P. Dubal*[,b,c]

[a]Department of Chemistry, Tarbiat Modares University, P.O. Box 14115-175, Tehran, Iran

[b]Centre for Materials Science, Queensland University of Technology (QUT), 2 George Street, Brisbane, QLD 4001, Australia

[c]School of Chemistry and Physics, Queensland University of Technology (QUT), 2 George Street, Brisbane, QLD 4001, Australia

*E-mail: morsali_a@modares.ac.ir (A. Morsali); deepak.dubal@qut.edu.au (D. P. Dubal).

**Materials and physical techniques.** All starting materials for the synthesis were purchased from commercial providers and used without further purification. FT-IR spectra were recorded using a Nicolet Fourier Transform IR 100 spectrometer in the 400-4000 $cm^{-1}$ range using the KBr disk technique. The thermal behavior of the samples was analyzed by a PL-STA 1500 apparatus working under a nitrogen atmosphere and at the heating rate of 10 °C $min^{-1}$. Powder X-ray diffraction (PXRD) measurements were performed using a Bruker AXS model D8 advanced with monochromated Cu-Kα (λ=1.54056 A) radiation. The $N_2$ adsorption/desorption isotherms were measured at 77 K using a Micromeritics ASAP 2020 analyzer. The specific surface area was calculated by the Brunauer-Emmett-Teller (BET) method. The inductively coupled plasma (ICP) analysis was performed on a Varian ICP-OES VISTA-PRO CCD instrument. A CHNS Thermo Scientific Flash 2000 elemental analyzer was used to analyze elemental contributions to the samples. Finally, melting points were measured on an Electrothermal 9100 apparatus.

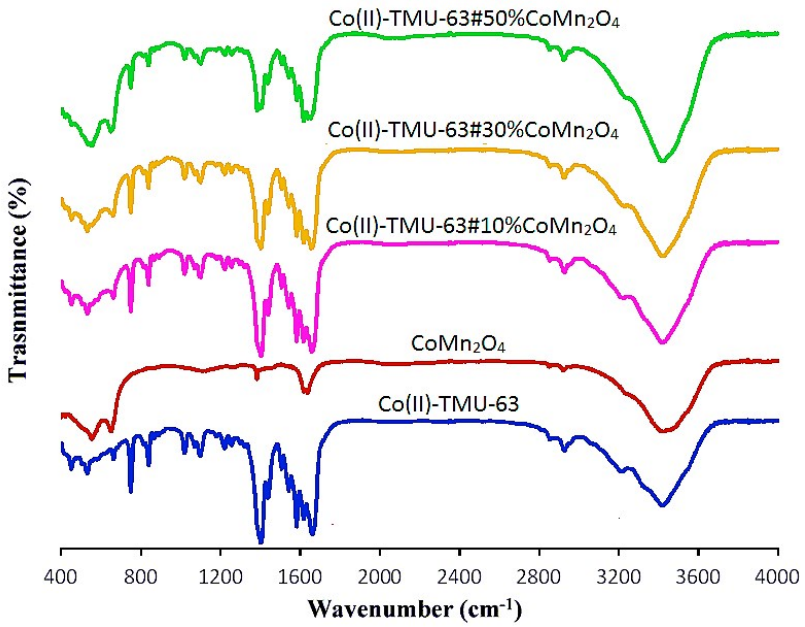


**Figure S1**. FT-IR spectra of the Co(II)-TMU-63, $CoMn_2O_4$, and Co(II)-TMU-63#X$CoMn_2O_4$ (X= 10, 30, and %50) NCPs.

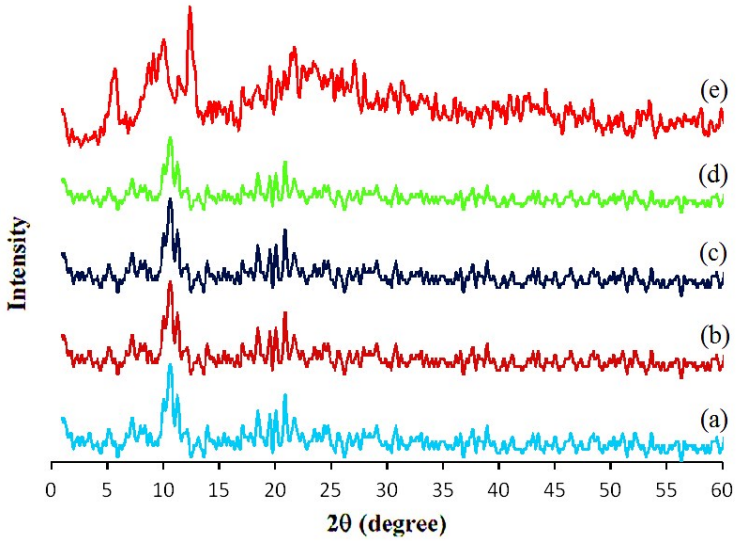


**Figure S2.** PXRD patterns of Co(II)-TMU-63 at different temperatures (a) 25 ℃, (b) 100 ℃, (c) 200 ℃, (d) 300 ℃, and (e) 350 ℃.

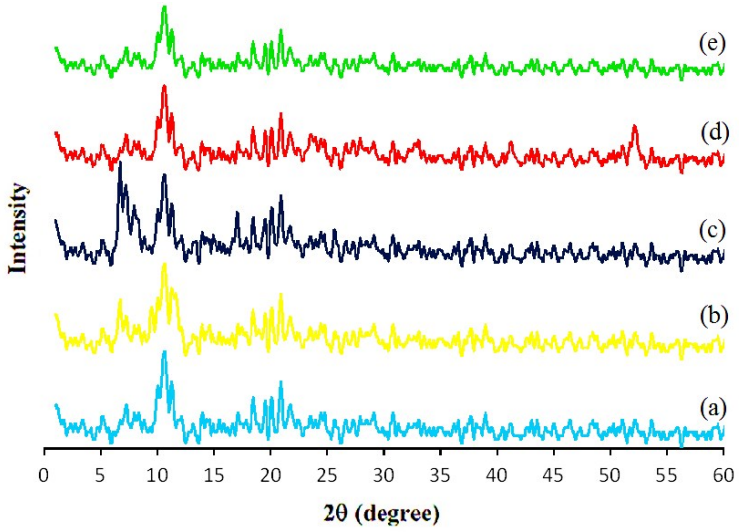


**Figure S3.** PXRD patterns of Co(II)-TMU-63 after refluxing for 24 h in different solvents (a) DMF, (b) acetonitrile, (c) *n*-hexane, (d) absolute ethanol, and (e) dimethyl sulfoxide.

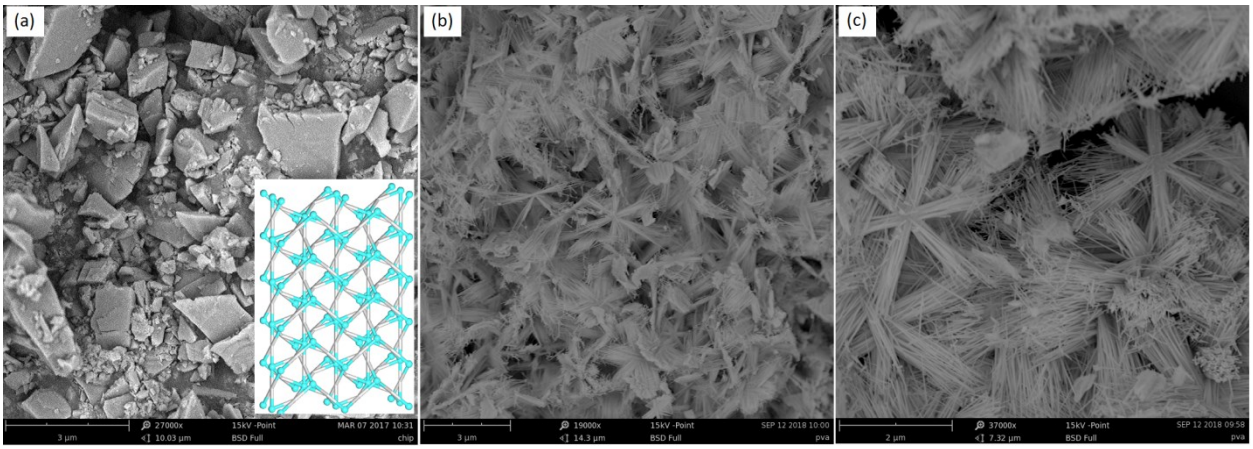


**Figure S4**. The FE-SEM images of (a) Co(II)-TMU-63, (b) Co(II)-TMU-63#10%$CoMn_2O_4$ NCPs, and (c) Co(II)-TMU-63#50%$CoMn_2O_4$ NCPs.

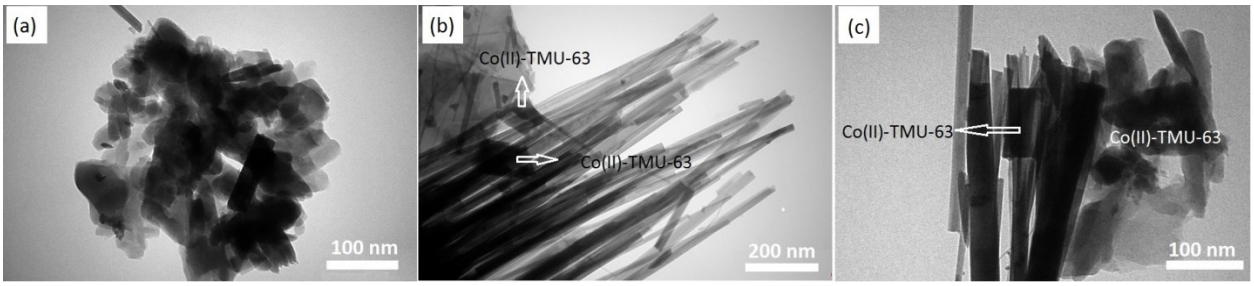


**Figure S5.** The TEM images of (a) Co(II)-TMU-63, (b) Co(II)-TMU-63#10%$CoMn_2O_4$ NCPs, and (c) Co(II)-TMU-63#50%$CoMn_2O_4$ NCPs.

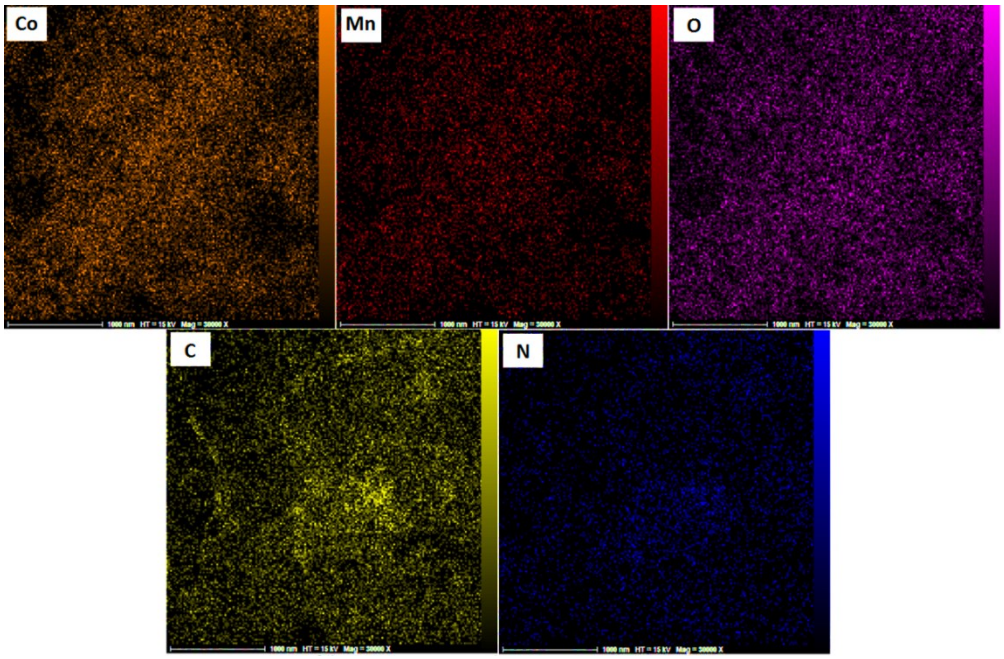


**Figure S6.** The elemental mapping of Co(II)-TMU-63#30%$CoMn_2O_4$ NCPs.

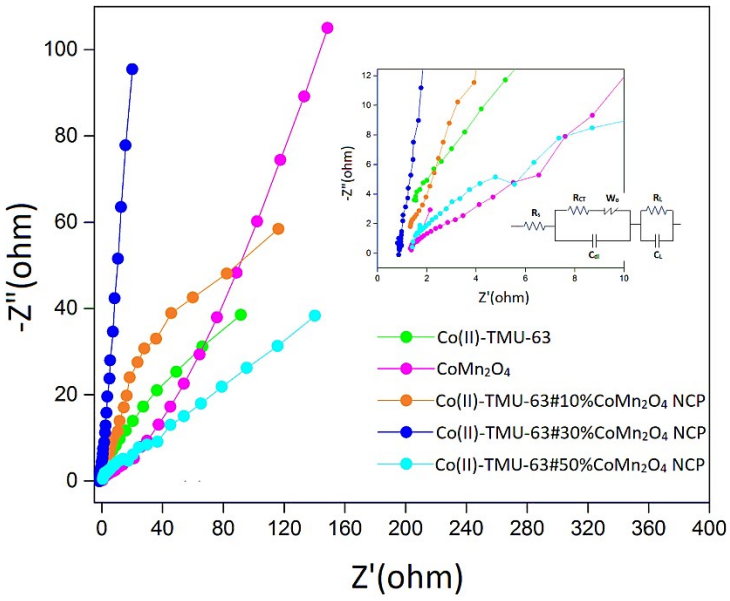


**Figure S7.** EIS Nyquist plots of electrode materials. Inset of figure including enlarged view of the Nyquist plots at high frequency range and the related circuit model.

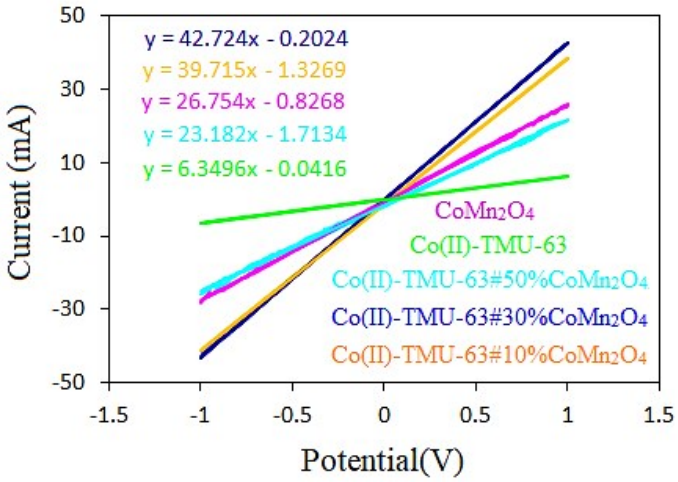


**Figure S8**. CV curves of electrode materials at a scan rate of 100mVs$^{-1}$.

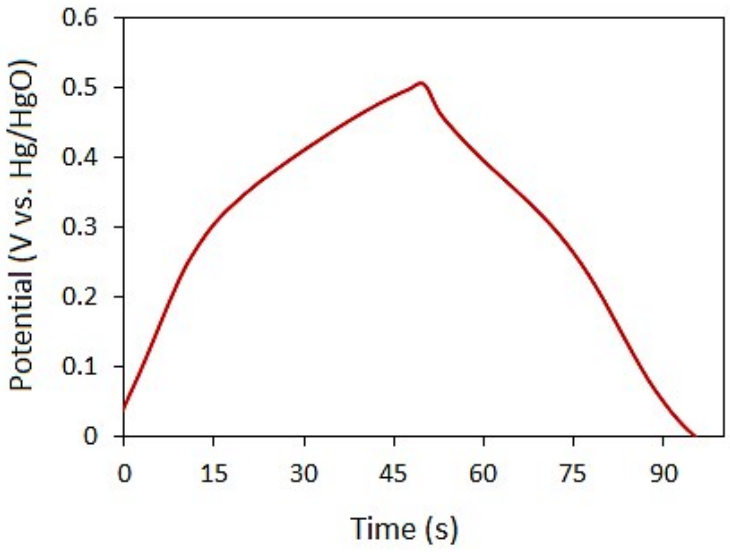


**Figure S9.** Charge-discharge curve of AC in a three electrode system.

**Table S1**. $R_s$ and $R_{ct}$ parameters obtained from EIS results for electrode materials.

| Electrode Material | $R_{CT}$ (Ω) | $R_s$ (Ω) |
|---|---|---|
| $CoMn_2O_4$ | 0.3 | 1.3 |
| Co(II)-TMU-63 | 0.25 | 1.3 |
| Co(II)-TMU-63#10%$CoMn_2O_4$ | 0.4 | 1.1 |
| Co(II)-TMU-63#30%$CoMn_2O_4$ | — | 0.9 |
| Co(II)-TMU-63#50%$CoMn_2O_4$ | 0.95 | 1.35 |